

Correlation of In Vivo DWI Injury Patterns with Finite Element Analysis of Mouse Spinal Cord Injury

T-W. Tu^{1,2}, P. V. Bayly¹, and S-K. Song²

¹Mechanical, Aerospace and Structural Engineering, Washington University in St. Louis, Saint Louis, MO, United States, ²Radiology, Washington University in St. Louis, Saint Louis, MO, United States

Introduction

Finite element analysis (FEA) overcomes the limit of direct measurement to study the mechanics of spinal cord injury (SCI)¹. The accurate representation of material properties is crucial to the validity of FEA. However, the material properties *in vivo* are difficult to measure. The lack of knowledge of tissue properties *in vivo* has posed a significant impediment to the application of FEA results to living tissue. In the present study, we employed diffusion MRI to assess the extent of SCI² correlation with the stress-strain predictions of a FEA model. The correlation will be used to refine the material properties for a better FEA modeling.

Material and Methods

Contusion Spinal Cord Injury

Ten- to twelve-week-old female transgenic thyl-YFP-16 mice, each weighing 19 - 22 g, underwent naïve *in vivo* scan before injury. Afterward, a controlled T9 contusion SCI was induced by the modified Ohio State University (OSU) impactor at a depth of 0.8 mm, and speed of 0.2 m/s. The animal was imaged in the hyper-acute phase (~3 hrs) to evaluate GM and WM integrity.

In vivo Diffusion MRI

Two-direction DWI, $(G_x, G_y, G_z) = (1, 1, 0), (0, 0, 1)$, was performed to probe the GM and WM structure using a multiple spin echo DWI sequence at *in vivo* resolution of $75 \mu\text{m} \times 75 \mu\text{m} \times 500 \mu\text{m}$. Imaging parameters are: TR ~1200 ms, TE 28 ms, TE2 15 ms, Δ 21 ms, δ 7 ms; b-value 0 and 1500 s/mm², FOV $1 \times 1 \text{ cm}^2$, data matrix 128×128 zero-filled to 256×256 , and 8 averages. The total scan time was 1.5 hr.

Finite Element Modeling of Contusion Spinal Cord Injury

The commercial FEA software package, ABAQUS, was used to create the FEA model based on *in vivo* DWI. *Ex vivo* experimental values for material properties obtained from Maikos (2008)¹, and Ichihara (2001)³ were first applied in the calculation. The Ogden and Mooney-Rivlin hyperelastic model was applied for spinal cord and CSF, respectively, as well as the appropriate boundary conditions, used previously in the literature¹.

Results

Structures of transverse T9 mouse spinal cord were segmented using D_{\perp} map for FEA model (Fig.1). The FEA model converged and provided estimates of the distribution of stress and strain during impact. From the DWI images (methods previously reported⁵) a decrease in axonal injury-induced D_{\parallel} , and increased hemorrhage-related T2 hypo-intensity was observed (Fig. 2).

The FEA-predicted stress and strain rate change patterns are consistent with GM and WM injury patterns shown in DWI (Fig. 3). In the initial impact (Phase I), the indentation produces a focal stress and strain rate change in the epicenter GM and WM resulting in GM hemorrhage and axonal stretch (Fig.3b). During the withdrawal of the impactor after impact (Phase II), the stress propagates, extending to the spinal cord remote from the epicenter. This may be related to secondary hemorrhage at the remote site (Fig. 3c). The stretch, i.e., strain rate, is still constrained focally at the epicenter.

Discussions and Conclusions

Consistent with previous reports^{3,4}, our preliminary data suggest that WM is more sensitive to strain-related changes, while the stress seems to affect GM. Although it is non-ideal to employing *in vitro* tissue properties in the FEA model, the predicted stress and strain fields from simulation of contusion SCI correlate well with the injury patterns detected using *in vivo* diffusion MRI (Fig. 3). With high-resolution *in vivo* DWI, it may be possible to use the observed injury patterns to iteratively improve the estimates of material parameters for GM and WM in FEA models of the spine. The ability to use FEA to simulate SCI under various conditions and obtain accurate predictions of injury would be of great use in the development of preventive measures.

References

1. Maikos et al., Neurotrauma, 2008, 25: 795-816; 2. Kim et al., MRM, 2007, 58: 253-260; 3. Ichihara et al., Neurotrauma, 2001, 18:361-367. 4. Sparrey et al., Spine, 2008;33:E812-819. 5. Tu et al., Neurotrauma, 2009, Aug. (in press)

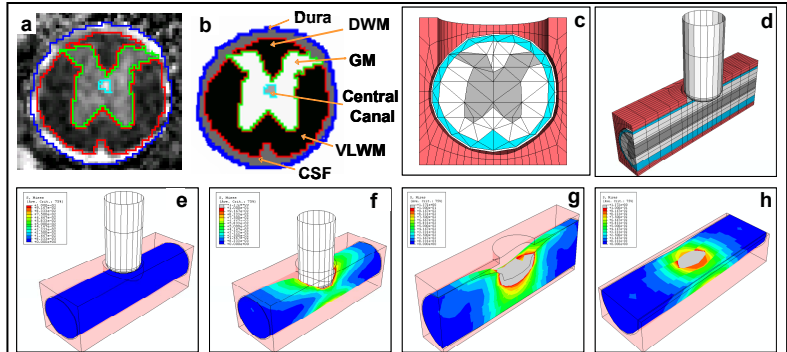


Figure 1. The FEA model consists of a spinal cord (with distinct element sets of GM, WM, CSF, and dura mater), a rigid spinal column and a rigid impactor. (a) bright WM and dark GM in D_{\perp} map, (b,c,d) DW-defined regions extracted for the FE mesh generation, (e-h) FEA modeling of the contusion SCI, representative results of the stress distribution of (g) coronal, and (h) sagittal view.

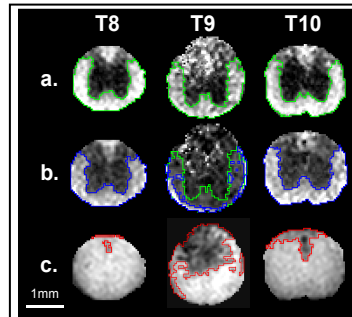


Figure 2. The injury patterns in the hyper-acute T2W/DWI maps in the epicenter (T9) and remote sites (T8 and T10): (a) AI maps provide contrast between GM and WM allowing total VWM (green) estimation, even in the injured cords. (b) D_{\parallel} maps show the axonal injury pattern as the decreased D_{\parallel} (the blue ROI denotes spared WM; the green ROI indicates total WM). (c) T2W images show the regions of GM and dorsal WM hematomas.

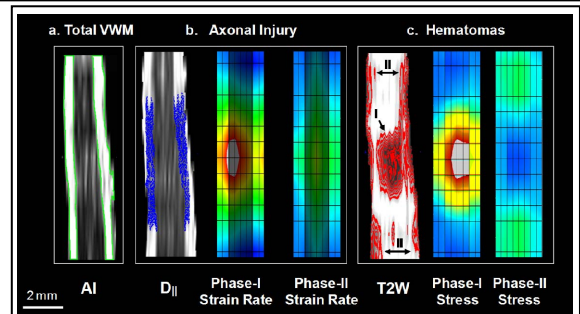


Figure 3. Comparison of coronal DWI maps and FEA contours on neuronal and axonal injury. (a) The total VWM after injury identified in AI map. (b) Axonal injury is mainly strain rate-related^{3,4}. The axonal injury identified in D_{\parallel} map (blue) corresponds to both strain-rate changes in Phases I and II. The regions of GM in FEA contours are blackened out for better observations of VWM. (c) In contrast, the stress propagation at the two Phases resulted in hematomas at both epicenter and remote sites. The primary mechanical factor for the neuronal disruption is stress⁴. The regions showing hematomas are marked in red by the signal intensity threshold in T2W image.